THE ASTROPHYSICAL JOURNAL, 572:L75–L78, 2002 June 10

A TIDALLY INTERACTING DISK IN THE YOUNG TRIPLE SYSTEM WL 20?

MARY BARSONY[1,2]
Jet Propulsion Laboratory, California Institute of Technology, MS 169-327, 4800 Oak Grove Drive, Pasadena, CA 91109; fun@uhuru.jpl.nasa.gov
THOMAS P. GREENE[2]
NASA Ames Research Center, MS 245-6, Moffett Field, CA 94035-1000; tgreene@mail.arc.nasa.gov
AND
GEOFFREY A. BLAKE
Division of Geological and Planetary Sciences, California Institute of Technology, MS 150-21, Pasadena, CA 91125; gab@gps.caltech.edu
Received 2002 March 26; accepted 2002 May 2; published 2002 May 14

ABSTRACT

We present high-resolution $\lambda = 2.7$ mm imaging of the close triple pre–main-sequence system WL 20. Compact dust emission with integrated flux density of 12.9 ± 1.3 mJy is associated with two components of the triple system, WL 20W and WL 20S. No emission above a 3 σ level of 3.9 mJy is detected toward the third component, WL 20E, which lies 3.″17 (400 AU) due east in projection from its neighbors. A possibly warped structure of $\sim 0.1\ M_\odot$ and $\leq 3.''2$ extent encompasses WL 20W and WL 20S, which have a projected separation of 2.″25 ($\sim$280 AU) along a north-south axis. This structure is most likely a tidally disrupted disk surrounding WL 20S. New near-infrared spectra of the individual components show a remarkable similarity between the two T Tauri stars of the system: WL 20E has a K7 spectral type ($T_{\rm eff} = 4040$ K) with $r_K = 0.2$, and WL 20W has an M0 spectral type ($T_{\rm eff} = 3800$ K) with $r_K = 0.2$. The spectrum of WL 20S is consistent with that of a source intrinsically similar to WL 20W, with $r_K < 0.9$, but seen through an $A_V = 25$ *in addition* to the $A_V = 16.3$ to the system as a whole. Taken together, these millimeter and infrared data help explain the peculiar nature of the infrared companion, WL 20S, as resulting from a large enhancement in its dusty, circumstellar environment in relation to its companions.

Subject headings: binaries: close — circumstellar matter — stars: formation — stars: individual (WL 20) — stars: pre–main-sequence

1. INTRODUCTION

WL 20 is a young triple system in the ρ Ophiuchi cloud core, consisting of two T Tauri stars (TTSs) and an object that exhibits the infrared spectral energy distribution (SED) characteristic of a late-stage, self-embedded protostar (Wilking & Lada 1983; Strom, Kepner, & Strom 1995; Ressler & Barsony 2001). The TTSs, WL 20E and WL 20W, have a projected linear separation of 400 AU (3.″17 at position angle [P.A.] 270°) at our adopted 125 ± 25 pc distance to the cloud (Knude & Hog 1998). The red object, WL 20S, is at a projected linear separation of just 280 AU from its nearest neighbor, WL 20W (2.″26 at P.A. 173°). Previously published mass estimates for the three young stellar objects (YSOs) are $\sim 0.65\ M_\odot$ for WL 20E, $0.53\ M_\odot$ for WL 20W, and $\geq 0.9\ M_\odot$ for WL 20S (Ressler & Barsony 2001). Given these masses and separations, the WL 20 system is expected to be dynamically unstable (Smith, Bonnell, & Bate 1997).

WL 20S exhibits additional peculiar properties, such as large amplitude variability over timescales of years (a factor of 3 in the near-IR and a factor of 6 in the mid-infrared), associated centimeter-wave continuum emission (Leous et al. 1991), and a resolved mid-infrared emitting region ~40–50 AU in diameter, whose size is constant over $12.5\ \mu{\rm m} \leq \lambda \leq 24.5\ \mu$m wavelengths. Taken together, these phenomena are consistent with the presence of enhanced, ongoing accretion activity in WL 20S.

Owing to their proximity, these three YSOs must have formed out of a single collapsing prestellar core and are therefore expected to be coeval to within a few times 10^4 yr. The derived age of each TTS, obtained by placement on the Hertzsprung-Russell diagram and comparison with isochrones from pre–main-sequence evolutionary tracks, is $\sim 2 \times 10^6$ yr. This age seems to be at odds with the appearance of WL 20S, which, although it could not be placed on an H-R diagram directly, lacking any previously available spectroscopy, otherwise has properties that would lead its age determination to be of order 10^5 yr old, were it observed to be in complete isolation.

One possible solution to this apparent age discrepancy is that accretion has continued into a late evolutionary phase in WL 20S owing to tidal interactions with its nearest neighbor, WL 20W (Ressler & Barsony 2001). In order to test this hypothesis directly, and to gain further insight into the nature of each individual YSO, we have obtained spatially resolved near-IR spectra of all three YSOs using NIRSPEC on Keck II and millimeter interferometric images using the Owens Valley Radio Observatory (OVRO).

2. OBSERVATIONS AND DATA REDUCTION

WL 20 was observed with all six 10.4 m diameter antennas of the Owens Valley Millimeter Array in 2001 in the 2.7 mm continuum in three configurations (L+E+H). Average single-sideband system temperatures at 110 GHz were 700–1000 K. Amplitude and phase calibration relied on observations of the nearby quasar, J1622−253, every 20 minutes, resulting in an absolute positional uncertainty of ~0.″2. Flux densities are based on observations of 3C 273, with an estimated uncertainty in

[1] Space Science Institute, 3100 Marine Street, Suite A353, Boulder, CO 80303-1058.

[2] Visiting Astronomer at the W. M. Keck Observatory, which is operated as a scientific partnership among the California Institute of Technology, the University of California, and the National Aeronautics and Space Administration. The Observatory was made possible by the generous financial support of the W. M. Keck Foundation.

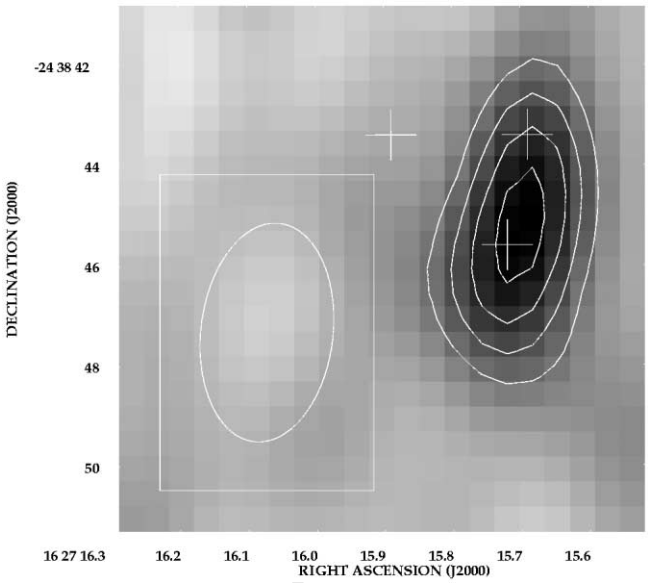

FIG. 1*a*

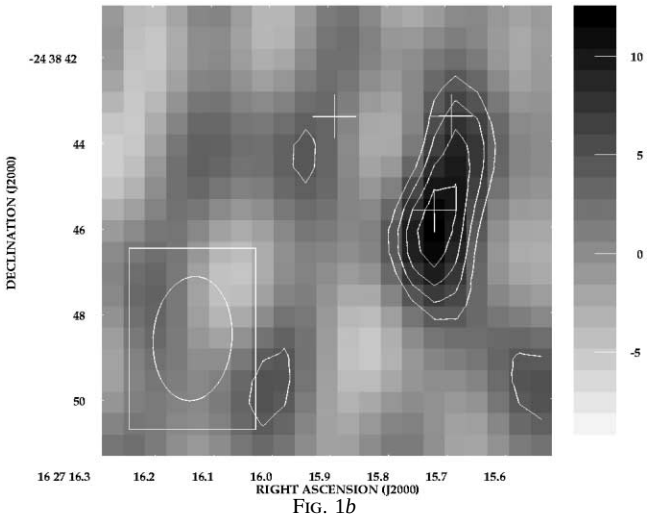

FIG. 1*b*

FIG. 1.—(*a*) 2.7 mm continuum image of the WL 20 triple system constructed from L+E+H configuration data. The beam (FWHM 4.″4 × 2.″6 at P.A. −7.°0) is indicated in the lower left corner. Contour levels are placed at 2, 3, 4, and 5 × 2 mJy beam^{-1}. The integrated flux in this figure is 12.9 ± 1.3 mJy. The locations of the infrared sources are indicated by the white crosses: WL 20E (R.A. = $16^h27^m15^s.89$, decl. = −24°38′43.″4 [J2000.0]), WL 20W (R.A. = $16^h27^m15^s.69$, decl. = −24°38′43.″4), and WL 20S (R.A. = $16^h27^m15^s.72$, decl. = −24°38′45.″6). (*b*) 2.7 mm continuum image of the WL 20 triple system from H-configuration data alone. The beam (FWHM 2.″9 × 1.″8 at P.A. −4.5) is indicated in the lower left corner. Contour levels are placed at 2, 3, 4, and 5 times the 2 mJy beam^{-1} noise level. Note the warping of the dust structure at this higher angular resolution.

the absolute fluxes of ∼20%. Raw data were calibrated and edited with the MMA software package (Scoville et al. 1993). Maps were created with the AIPS[3] package of NRAO, using the MX task.

All near-IR (2.06–2.49 μm) spectra were acquired through clouds on 2001 June 14 UT using the NIRSPEC facility spectrograph (McLean et al. 1998) on the 10 m Keck II telescope atop Mauna Kea, Hawaii. NIRSPEC was used in low-resolution mode with a 0.″38 (2 pixel) wide, 42″ long slit, providing spectral resolution $R \equiv \lambda/\delta\lambda = 2200$. WL 20E and W were observed simultaneously in the slit (oriented with a 90° P.A.), and WL 20S was observed separately. Each exposure was 200 s, and each object was observed in four exposures (including nodded frames) for a total of 800 s each. The A0 V star HIP 79229 was observed within 0.1 air mass of the WL 20 components, and it was used for telluric correction. Spectra of the internal NIRSPEC continuum lamp were taken for flat fields, and exposures of its Ar, Ne, Kr, and Xe lamps were used for wavelength calibrations.

All near-IR spectra were reduced with IRAF.[4] First, object and sky frames were differenced and then divided by flat fields. Next, bad pixels were fixed via interpolation, and spectra were extracted with the APALL task. Spectra were wavelength-calibrated using low-order fits to lines in the arc lamp exposures, and spectra at each slit position of each object were co-added. Instrumental and atmospheric features were removed by dividing wavelength-calibrated object spectra by spectra of HIP 79229 (which had their 2.166 μm H Brγ absorptions removed). Combined spectra were produced by summing the spectra of both slit positions for each object. Finally, the spectra were multiplied by an artificial spectrum of a $T = 10{,}000$ K blackbody in order to restore their true continuum slopes and they were normalized to 1.0.

[3] AIPS is produced and maintained by the National Radio Astronomy Observatory, a facility of the National Science Foundation operated under cooperative agreement by Associated Universities, Inc.

[4] IRAF is distributed by the National Optical Astronomy Observatories, which are operated by the Association of Universities for Research in Astronomy, Inc., under cooperative agreement with the National Science Foundation.

3. RESULTS

We present the 2.7 mm continuum images of the WL 20 triple system in Figure 1. The white crosses mark the positions of the infrared counterparts of the three YSOs: WL 20E, WL 20W, and WL 20S. Absolute astrometric positions for WL 20E ($K = 10.13$) and WL 20W ($K = 10.40$) are from the Two Micron All Sky Survey (2MASS) database and are estimated to be accurate to 0.″2. The position of WL 20S (unresolved from its brighter neighbors by 2MASS at $K = 12.6$) is then deduced by relative astrometry from the mid-infrared, accurate to ≈0.″02 (Ressler & Barsony 2001).

Figure 1*a* shows the (combined L+E+H configuration) continuum image of the WL 20 triple system. The total flux in this image is 12.9 ± 1.3 mJy. The observed dust structure, modeled as an elliptical Gaussian centered on the emission peak, has a projected major axis of 5.″2 ± 0.″5 at P.A. = 172° ± 5° and a minor axis of width 2.″6 ± 0.″2. Figure 1*b* shows just the high-resolution (H configuration) continuum image which has an integrated flux of 14.2 ± 2.4 mJy. The extent of the major axis of the elongated emission feature is 3.″8 ± 0.″7, if modeled as an elliptical Gaussian, with P.A. = 172° ± 7°, with a minor axis of 1.″5 ± 0.″3 extent.

The reduced WL 20 component spectra are shown in Figure 2. The WL 20E and W spectra both have signal-to-noise ratios (S/Ns) of approximately 100, while the WL 20S value is S/N ∼ 10. The spectra of WL 20E and W are nearly identical and are consistent with late-type dwarf or pre–main-sequence stars with little veiling. Identification and measurements of the diagnostic photospheric absorption features from the spectra of WL 20E and W are listed in Table 1.

We have derived the spectral types and veilings of WL 20E and W by comparing their spectra to those of dwarf MK

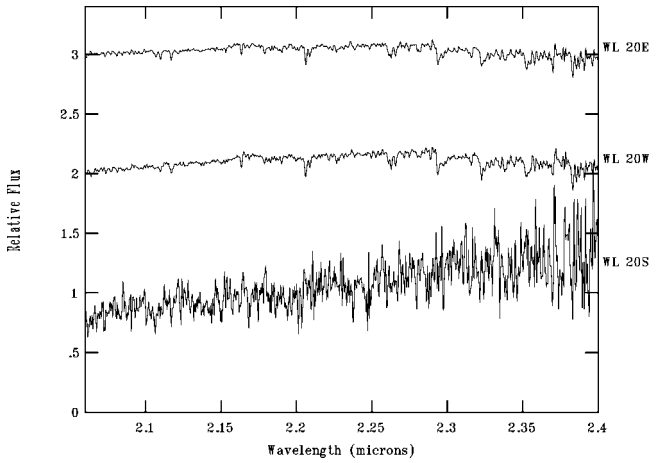

FIG. 2.—NIRSPEC spectra of the components of WL 20. The spectra of WL 20E and W are nearly identical and consistent with that of late-type dwarf or pre–main-sequence stars with little veiling. However, the 2.28 μm feature is stronger in WL 20E, indicating that it is of slightly earlier spectral type. The spectrum of WL 20S shows no absorption features (perhaps because of its low signal-to-noise ratio), but its red shape indicates that it suffers considerably more extinction than either WL 20E or W (see text for details).

standards also taken with NIRSPEC. We used the veiling-independent ratio of the 2.21 and 2.28 μm region features to derive a K7 IV/V spectral type for WL 20E and an M0 IV/V spectral type for WL 20W. Similarly, we derive veilings $r_k = 0.2$ for both WL 20E and W by comparing the measured equivalent widths of their 2.21 μm features to those of standard stars of the same spectral types. The spectral types of these objects translate into effective temperatures of 4040 and 3800 K for WL 20E and W, respectively, assuming a dwarf temperature scale (Tokunaga 2000). These classifications are uncertain to approximately one spectral subclass ($\Delta T_{\rm eff} \simeq 200$ K), and Luhman & Rieke (1999) found very similar results for these two objects.

The WL 20S spectrum shows no obvious absorption or emission features, but its shape can be used to investigate its circumstellar environment. The steep, red slope of its spectrum is similar to the spectral slopes of Class I YSOs in this wavelength region (Greene & Lada 1996). If WL 20S has the same intrinsic spectrum and K flux as WL 20W, then its spectrum can be matched by extinguishing the spectrum of WL 20W by an *additional* $A_v = 25$ mag. This amount of extinction is also approximately consistent with the $\delta K = 2.2$ mag brightness difference of these two objects. These spectral shape and brightness properties make it unlikely that WL 20S has a large amount of excess 2 μm emission. If WL 20S had a large 2 μm excess and greater extinction (i.e., to match its observed K flux), then its spectrum would have a steeper slope and more apparent extinction than consistent with the K-band flux difference between it and WL 20W. The measured flux difference and spectra limit the amount of this excess to $r_k < 0.9$ from relative comparison with WL 20W, consistent with the spectrum not showing a strong 2.166 μm H Brγ emission line.

4. DISCUSSION

One possible explanation for the peculiar properties of WL 20S relative to its northern neighbors is a chance superposition of sources. If WL 20S were not physically associated with this system, then it could be in any evolutionary state whatsoever relative to WL 20E and W. Figure 1 clearly rules out this possibility, since both WL 20W and WL 20S lie within the same compact dust emitting region, proving a physical association. This leaves the presence of enhanced circumstellar material around WL 20S, perhaps associated with enhanced accretion activity, as the most plausible explanation for its peculiar appearance.

TABLE 1
NIRSPEC PHOTOSPHERIC ABSORPTION LINE STRENGTHS

SPECTRAL FEATURE SPECIFICATION	SPECTRAL FEATURE WAVELENGTHS (μm)	MEASURED EQUIVALENT WIDTHS (Å)	
		WL 20E	WL 20W
Na doublet	2.206 and 2.209	3.1 ± 0.1	3.2 ± 0.1
Ca triplet	2.261, 2.263, and 2.266	4.2 ± 0.1	4.2 ± 0.1
CO band heads	2.29 and 2.32	11 ± 1.5	13 ± 1.5
Mg, Ca, and Fe	2.28	1.4 ± 0.1	0.9 ± 0.1

Previous single-telescope observations toward WL 20 at 1.3 mm in an 11″ beam measured a flux of 95 mJy but could not localize the emission source(s) (André & Montmerle 1994; Motte, André, & Neri 1998). Under the assumption that disk emission could account for all of the observed 1.3 mm flux, using a spectral slope $\alpha = 2.5$ ($S_\nu \propto \nu^\alpha$), appropriate for accretion disks (Hogerheijde 1998), the expected 2.7 mm continuum flux from the WL 20 system is 15 mJy. This is to be compared with the total measured flux of 12.9 ± 1.3 mJy from Figure 1*a*. Our data are, therefore, consistent with the hypothesis that all of the observed millimeter emission from the WL 20 system originates from a compact disk structure, with negligible emission from any envelope component. Assuming optically thin dust emission at $T_d = 50$ K, and a gas-to-dust ratio of 100 by mass, the observed millimeter flux corresponds to a mass of 0.1 $M_\odot$ for $\kappa_{1.3\ {\rm mm}} = 0.1$ cm^2 g^{-1} (Ossenkopf & Henning 1994).

It is clear from both Figures 1*a* and 1*b* that no millimeter continuum emission is associated with WL 20E to our sensitivity limit of 3.9 mJy (3 σ), which corresponds to a disk mass upper limit of $\sim 2.4 \times 10^{-2}$ $M_\odot$ for an assumed optically thin, constant $T = 50$ K dust temperature source. This finding is consistent with the appearance of the near-IR spectrum of WL 20E, which exhibits only slight continuum veiling (see Fig. 2).

It is difficult to distinguish from the data presented in Figure 1 how much, if any, contribution the source, WL 20W, makes to the observed dust structure. One possible interpretation is that WL 20S possesses a large disk that is interacting with a smaller disk around WL 20W. We consider this scenario to be somewhat unlikely because near-IR photometry and spectra (Fig. 2) show that WL 20W has no more reddening or excess than WL 20E, implying that it does not have a substantial millimeter-emitting circumstellar disk.

The image of Figure 1*b* is highly suggestive of a tidally disrupted disk around WL 20S. The likely presence of such a disrupted disk was previously inferred on the basis of the appearance of the SED of WL 20S, which is consistent with presence of an ~250 AU radius disk (Chiang & Goldreich 1999; Ressler & Barsony 2001) of size comparable to the projected 280 AU separation between WL 20W and WL 20S. Since the interpretation of SEDs alone is nonunique, the imaging information presented here, when combined with the source SED, provides the first direct evidence for strong disk interaction in a young, dynamically evolving multiple system and resolves the apparent age discrepancy among its components.

Future higher spatial resolution imaging of the dust continuum structure surrounding WL 20S with the Combined Array for Research in Millimeter-wave Astronomy or the Atacama Large Millimeter Array could shed further insight into the na-

ture of the disk's interaction with its close neighbor, WL 20W. Kinematic studies await high-sensitivity and high-resolution submillimeter line imaging in species and transitions unaffected by foreground absorption.

We would like to thank Al Wootten, the staff at OVRO, Ralf Launhardt, and Adwin Boogert for help with OVRO data acquisition and reduction and for useful scientific discussions. The authors also extend special thanks to Marianne Takamiya for taking the NIRSPEC data and to NOAO for granting Gemini/NIRSPEC observing time. We wish to recognize and acknowledge the very significant cultural role and reverence that the summit of Mauna Kea has always had within the indigenous Hawaiian community. We are most fortunate to have the opportunity to conduct observations from this mountain. The Owens Valley millimeter-wave array is supported by NSF grant AST 99-81546. M. B. acknowledges financial support from NASA's Long Term Space Astrophysics Research Program, NAG5-8412.

REFERENCES

André, P., & Montmerle, T. 1994, ApJ, 420, 837
Chiang, E. I., & Goldreich, P. 1999, ApJ, 519, 279
Greene, T. P., & Lada, C. J. 1996, AJ, 112, 2184
Hogerheijde, M. 1998, Ph.D. thesis, Univ. Leiden
Knude, J., & Hog, E. 1998, A&A, 338, 897
Leous, J. A., Feigelson, E. D., André, P., & Montmerle, T. 1991, ApJ, 379, 683
Luhman, K. L., & Rieke, G. H. 1999, ApJ, 525, 440
McLean, I. S., et al. 1998, Proc. SPIE, 3354, 566
Motte, F., André, P., & Neri, R. 1998, A&A, 336, 150
Ossenkopf, V., & Henning, Th. 1994, A&A, 291, 943
Ressler, M. E., & Barsony, M. 2001, AJ, 121, 1098
Scoville, N. Z., Carlstrom, J. E., Chandler, C. J., Phillips, J. A., Scott, S. L., Tilanus, R. P. J., & Wang, Z. 1993, PASP, 105, 1482
Smith, K. W., Bonnell, I. A., & Bate, M. R. 1997, MNRAS, 288, 1041
Strom, K. M., Kepner, J., & Strom, S. E. 1995, ApJ, 438, 813
Tokunaga, A. T. 2000, in Allen's Astrophysical Quantities, ed. A. N. Cox (4th ed.; New York: Springer), 143
Wilking, B. A., & Lada, C. J. 1983, ApJ, 274, 698